Cell, Vol. 123, 463–475, November 4, 2005, Copyright ©2005 by Elsevier Inc. DOI 10.1016/j.cell.2005.08.041

Calibrated Measurement of Gating-Charge Arginine Displacement in the KvAP Voltage-Dependent K^+ Channel

Vanessa Ruta, Jiayun Chen, and Roderick MacKinnon*
Howard Hughes Medical Institute
Laboratory of Molecular Neurobiology and Biophysics
Rockefeller University
1230 York Avenue
New York, New York 10021

Summary

Voltage-dependent ion channels open and conduct ions in response to changes in cell-membrane voltage. The voltage sensitivity of these channels arises from the motion of charged arginine residues located on the S4 helices of the channel's voltage sensors. In KvAP, a prokaryotic voltage-dependent K^+ channel, the S4 helix forms part of a helical hairpin structure, the voltage-sensor paddle. We have measured the membrane depth of residues throughout the KvAP channel using avidin accessibility to different-length tethered biotin reagents. From these measurements, we have calibrated the tether lengths and derived the thickness of the membrane that forms a barrier to avidin penetration, allowing us to determine the magnitude of displacement of the voltage-sensor paddles during channel gating. Here we show that the voltage-sensor paddles are highly mobile compared to other regions of the channel and transfer the gating-charge arginines 15–20 Å through the membrane to open the pore.

Introduction

The activity of voltage-dependent ion channels underlies the rapid, long-range electrical signaling of the nervous system (Hille, 2001). These channels contain voltage sensors that regulate or "gate" the passage of ions through the pore depending on the value of the membrane voltage. This functional property endows voltage-dependent ion channels with the ability to generate action potentials and propagate them rapidly over the neuronal membrane. How is the membrane voltage "sensed" in these channels? Four voltage-sensing domains surround a central ion-conduction pore. Highly conserved basic amino acids termed "gating charges" are concentrated on the S4 segment of each voltage sensor. The S4 gating-charge residues move under the influence of the membrane's electric field, a voltage-dependent conformational change that is coupled to opening of the pore (Sigworth, 1994). Electrical measurements in the Shaker voltage-dependent K^+ (Kv) channel indicate that in total ~12-14 positive elementary charge units cross the membrane's electric field during channel activation (Schoppa et al., 1992; Aggarwal and MacKinnon, 1996; Seoh et al., 1996). The large valence of the gating charge contributes to the exquisite voltage-sensitivity of these channels, allowing them to gate open in response to small changes in the membrane voltage.

A detailed understanding of the mechanics of gating charge movement is essential in order to understand the structural basis of the voltage-dependent gating process. How S4 moves within the membrane's electric field has remained controversial. Different technical approaches have been used to measure the voltage-dependent motions of the S4 segment and have yielded conflicting conclusions on the extent that S4 moves, leading to widely disparate models of how S4 transfers gating charges across the membrane. In eukaryotic voltage-dependent ion channels, the motions of the S4 segment have been partially inferred from the accessibility of introduced cysteines to small hydrophilic thiol reactive compounds (Yang and Horn, 1995; Mannuzzu et al., 1996; Yang et al., 1996; Larsson et al., 1996; Yusaf et al., 1996; Baker et al., 1998). In these experiments, channel function was measured prior to and after treatment with thiol reactive compounds to evaluate the accessibility of S4 cysteine mutants. Most residues on the S4 segment of the Shaker Kv channel exhibit large changes in accessibility depending on whether the channel is in a closed or opened conformation. A stretch of 10 amino acids within the N-terminal half of S4 moves from an inaccessible to an externally accessible location with membrane depolarization while, at the same time, a stretch of 12 amino acids within the C-terminal half moves from an internally accessible to an inaccessible location (Larsson et al., 1996; Baker et al., 1998).

What does the extensive state-dependent accessibility of residues in the S4 segment tell us about the mechanism of gating-charge movement? A cysteine residue can react with a small hydrophilic thiol-reactive compound if the cysteine lies at the surface of the protein or if it lines a crevice formed within the membrane that would provide an aqueous pathway to allow diffusion of the compound to the cysteine sulfhydryl (Figure 1A). Thus, there are two possible explanations for the pervasive accessibility of residues on the S4 segment to small thiol-reactive compounds. The first is that the S4 segment translates a large distance (~15 Å) perpendicular to the plane of the membrane with membrane depolarization. The second interpretation, favored in many models of voltage-dependent gating, is that the S4 helix lies within deep aqueous crevices that penetrate the protein from both sides of the membrane and the state-dependent accessibility of introduced cysteines arises from rotations of the S4 helix, with little or no translational motion (Bezanilla, 2000; Gandhi and Isacoff, 2002). This latter interpretation attempts to reconcile the state-dependent accessibility of S4 residues with conclusions from luminescence resonance energy transfer (LRET) experiments that S4 undergoes only small transverse motions (Cha et al., 1999). Accessibility measurements using small thiol-reactive compounds cannot distinguish between these possible S4 motions.

*Correspondence: mackinn@rockefeller.edu

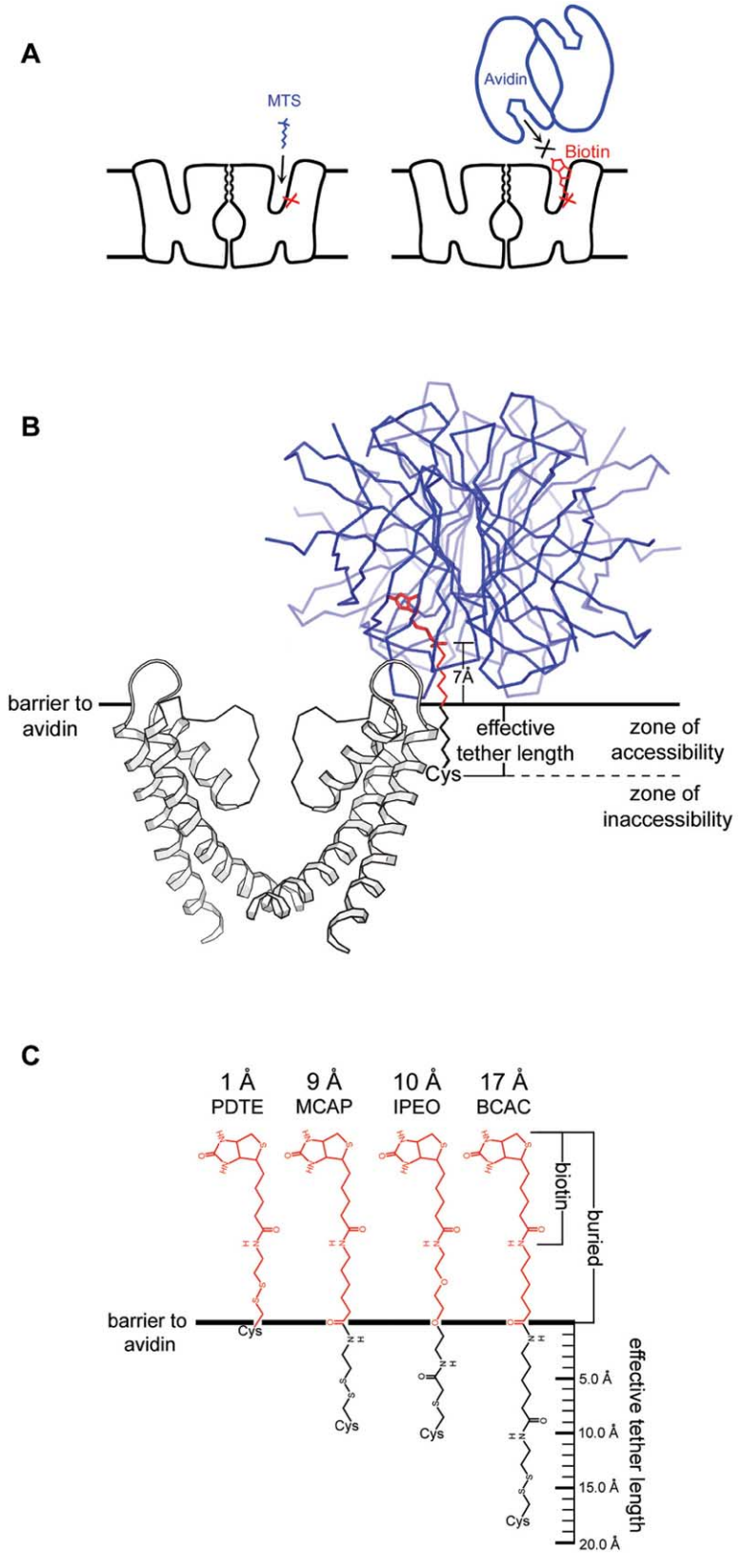

Figure 1. Using Tethered Biotin and Avidin to Measure the Depth of Channel Amino Acids within the Membrane

(A) Small hydrophilic thiol-reactive compounds like methanethiosulfonate (MTS) reagents can bind to a cysteine residue on the channel (red X) that lies within a crevice in the membrane (left). Avidin is too large to fit into crevices and so cannot bind a biotinylated cysteine residue if the tether is too short (right).

(B) The KvAP pore (two opposing subunits, white ribbon) is viewed from the side, with the approximate external membrane boundary that forms a barrier to avidin marked. A biotinylated cysteine residue on the channel can only bind avidin (blue wire, Cα trace) if the α-carbon of the cysteine residue lies within the effective tether length of the membrane surface (the zone of accessibility).

(C) Extended chemical structures of the tethered biotin reagents employed in this study. Biotin and ~7 Å of the tether become buried when bound to avidin (red). The remainder of the tether defines the effective tether length (black) for the biotin reagent.

An alternative approach to examine the topology and dynamics of channel proteins is to measure the accessibility of avidin to tethered biotin reagents linked to cysteine residues on the channel (Slatin et al., 1994; Qiu et al., 1996; Senzel et al., 1998; Jiang et al., 2003b). Avidin is a large rigid protein (Pugliese et al., 1993) (~56 by 50 by 40 Å) and so will not fit into crevices formed within the channel (Figures 1A and 1B). The accessibility of a biotinylated cysteine residue on the channel will therefore depend only on the length of the biotin tether and the depth of the cysteine residue below the surface of the membrane. Consequently, this accessibility technique has an advantage in that it can detect translational motions of the S4 segment relative to the membrane surface without the possibility of alternative interpretations.

In a previous study, this second approach was used to investigate the gating motions of the S4 segment in KvAP, a prokaryotic Kv channel (Jiang et al., 2003b). The crystal structure of KvAP revealed that the S4 segment forms part of a helix-turn-helix structure, termed the voltage-sensor paddle, located at the channel's outer perimeter (Jiang et al., 2003a). The voltage-sensor paddles are attached to the body of the channel through flexible connections, suggesting that the gating-charge residues might be carried through the membrane's electric field by the rigid-body motions of the paddles at the protein-lipid interface. This hypothesis for gating-charge movement was tested by labeling individual paddle residues with a single-length biotin tether and then evaluating the accessibility of the biotinylated residue to avidin in the solution on either side of the membrane. These functional experiments led to the proposal that the S4 segment translates a large distance (~20 Å) through the membrane, driven by the membrane voltage (Jiang et al., 2003b).

Here we use multiple biotin tethers of different lengths to measure the membrane depth of amino acids throughout the entire KvAP channel, including the pore and all four transmembrane segments of the voltage sensor. The measurements provide an internally consistent data set that tightly constrains the limits of amino acid depth change associated with channel gating. We find that the voltage-sensor paddle, and the S4 segment in particular, is a uniquely mobile part of the channel that moves the gating-charge arginine residues more than 15 Å through the membrane.

Results

Using Tethered Biotin to Measure Membrane Depth

A basic assumption underlying this analysis is that the protein avidin is too large and hydrophilic to penetrate beneath the surface of the membrane (Figure 1B). Therefore, in order for a biotinylated residue on the channel to be able to capture avidin in the solution outside the membrane, the α-carbon of the cysteine residue to which biotin is attached must lie within the effective tether length of the membrane surface (zone of accessibility, Figure 1B). Biotinylated cysteine residues that reside deeper beneath the membrane surface (zone of inaccessibility, Figure 1B) will be unable to capture avidin because the biotin tether will be too short to allow the biotin moiety to reach its binding site deep within the avidin protein. Thus, the binary outcome of accessibility or inaccessibility to avidin generates a distance constraint for the depth of the biotinylated residue within the membrane, relative to the membrane surface.

Figure 1C shows the chemical structure of the four biotin reagents used in this study. When bound to avidin, the biotin moiety plus an additional ~7 Å of the tether (colored red) will be buried within the binding pocket of avidin. Therefore, this region of the biotin tether must be positioned fully outside the membrane surface in order to allow avidin binding to occur (Figure 1B). The remainder of the tether, from the α-carbon of the cysteine to the surface of the avidin protein, defines the effective tether length of the biotin reagent (colored black, Figures 1B and 1C). We estimate the effective tether length to be ~1 Å for PDTE biotin, ~9 Å for MCAP biotin, ~10 Å for IPEO biotin, and ~17 Å for BCAC biotin. These distances correspond to the length of the maximally extended tether.

Calibration of Distances Using the Pore

Our goal is to determine the voltage-dependent displacement of components of the channel within the membrane when the channel gates. To accomplish this goal, we must first examine the assumption that the membrane is a strict barrier to avidin penetration and that the effective tether lengths do indeed correspond to their extended chemical structures, taking into account the dimensions of the biotin binding pocket inside avidin. Therefore, we used the KvAP pore, a rigid and essentially immobile (with respect to translation perpendicular to the membrane plane) part of the channel, whose structure and orientation within the membrane are known, to calibrate our measurement.

Single cysteine mutations were introduced into a cysteine-less KvAP channel. The cysteine mutant channels were expressed, purified in detergent, reacted with tethered biotin reagents, and reconstituted into planar membranes in order to evaluate avidin accessibility in the functioning channels. To detect avidin binding to biotinylated channels, we compared current records elicited by depolarization prior to and after addition of avidin to each side of the membrane. Because avidin is so large, we expect that, when it binds, it should have some detectable effect on channel function. This expectation turns out to be correct. Absolute rates of reactivity (avidin capture of tethered biotin) were variable at different sites on the channel. Even known surface-exposed positions can exhibit slow rates of reactivity (e.g., position Y173 on the turret outside S5, Figure 2A). Since many factors can influence the rates of reactivity, we simply want to know whether or not the reaction occurs. This binary assay reports accessibility: reactivity or nonreactivity tells us whether a biotinylated residue on the KvAP channel lies close enough to the surface of the membrane to be able to bind avidin or not.

Figure 3A shows representative experiments for a series of residues staggered along the length of the S5 helix. Control experiments show that avidin nonspecifically inhibits up to ~20% of channel current when added to the internal side of the membrane (Jiang et

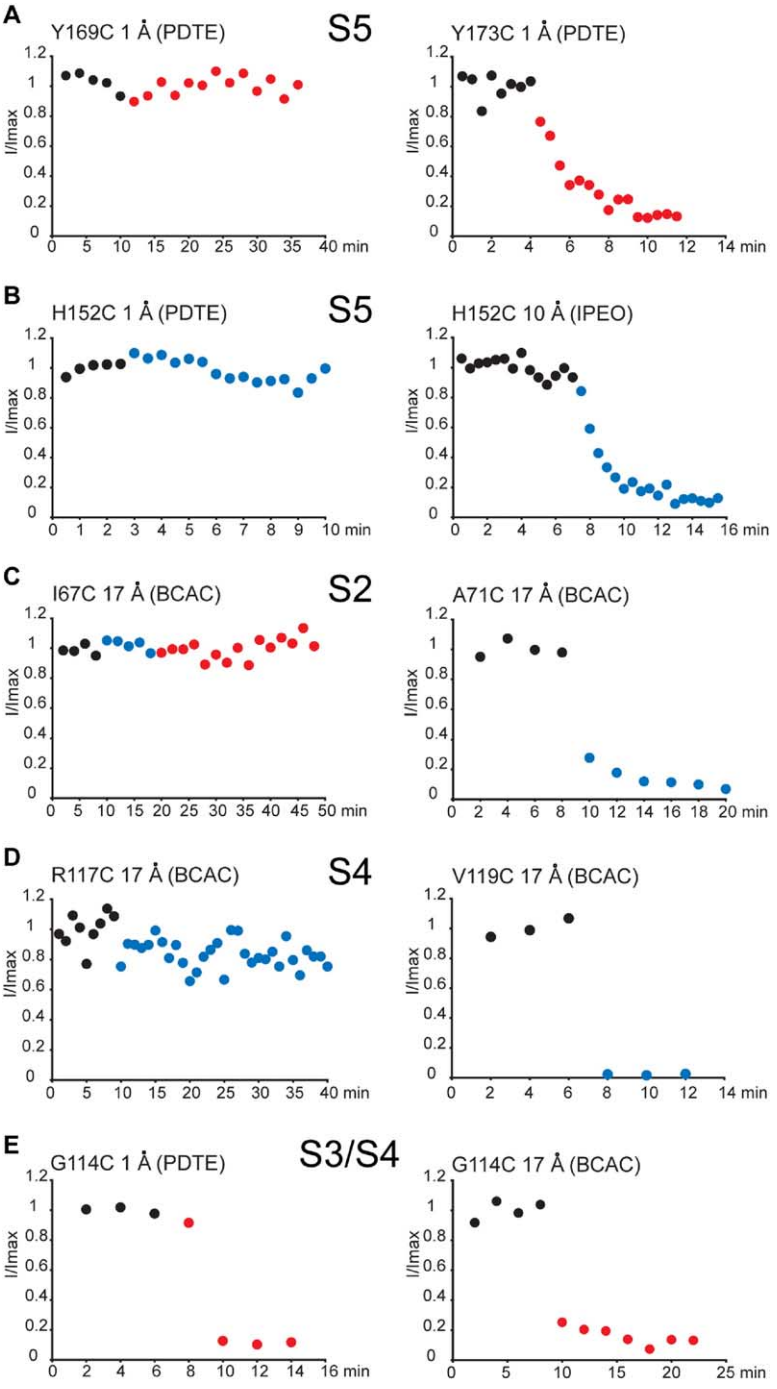

Figure 2. Avidin Binding to Biotinylated Channels Robustly Affects Channel Function

Currents were elicited by depolarization and normalized to the average control prior to (black circles) or after addition of external (red circles) or internal (blue circles) avidin.

(A) Comparison of the effect of external avidin on 2 nearby residues on S5, both labeled with the 1 Å biotin tether.

(B) Comparison of the effect of internal avidin on H152C on S5 labeled with a shorter (left) and longer (right) biotin tether.

(C) Comparison of the effect of avidin on 2 nearby residues on S2 labeled with the 17 Å biotin tether.

(D) Comparison of the effect of internal avidin on 2 nearby residues on S4 labeled with the 17 Å biotin tether.

(E) External avidin inhibits a paddle residue prior to depolarization when labeled with a 17 Å biotin tether (right) and only after depolarization when labeled with a 1 Å biotin tether (left).

al., 2003b). However, this nonspecific background inhibition does not obscure the robust functional effects that occur when avidin binds to biotinylated cysteine mutant channels, allowing us to differentiate readily between accessible and inaccessible sites (Figure 2).

As we move from sites at the N terminus to sites at the C terminus of S5 (see Figure 3), traversing the membrane, how does avidin accessibility change? At the N terminus of S5, I148C channels labeled with the 10 Å (IPEO) tether are completely inhibited by internal but not external avidin. I148C channels labeled with the short 1 Å (PDTE) tether are similarly inhibited by internal avidin, constraining this site to lie very near to the internal membrane boundary.

H152C lies one helical turn further into the membrane on S5. When H152C channels are labeled with the 10 Å (IPEO) tether, channel currents are again inhibited by internal avidin only. However, intracellular avidin has no effect on H152C channels when labeled with the 1 Å (PDTE) tether. This lack of effect is not due to deficient biotinylation, which was evaluated with protein gel assays for all cysteine mutants studied (see Figure S1 in

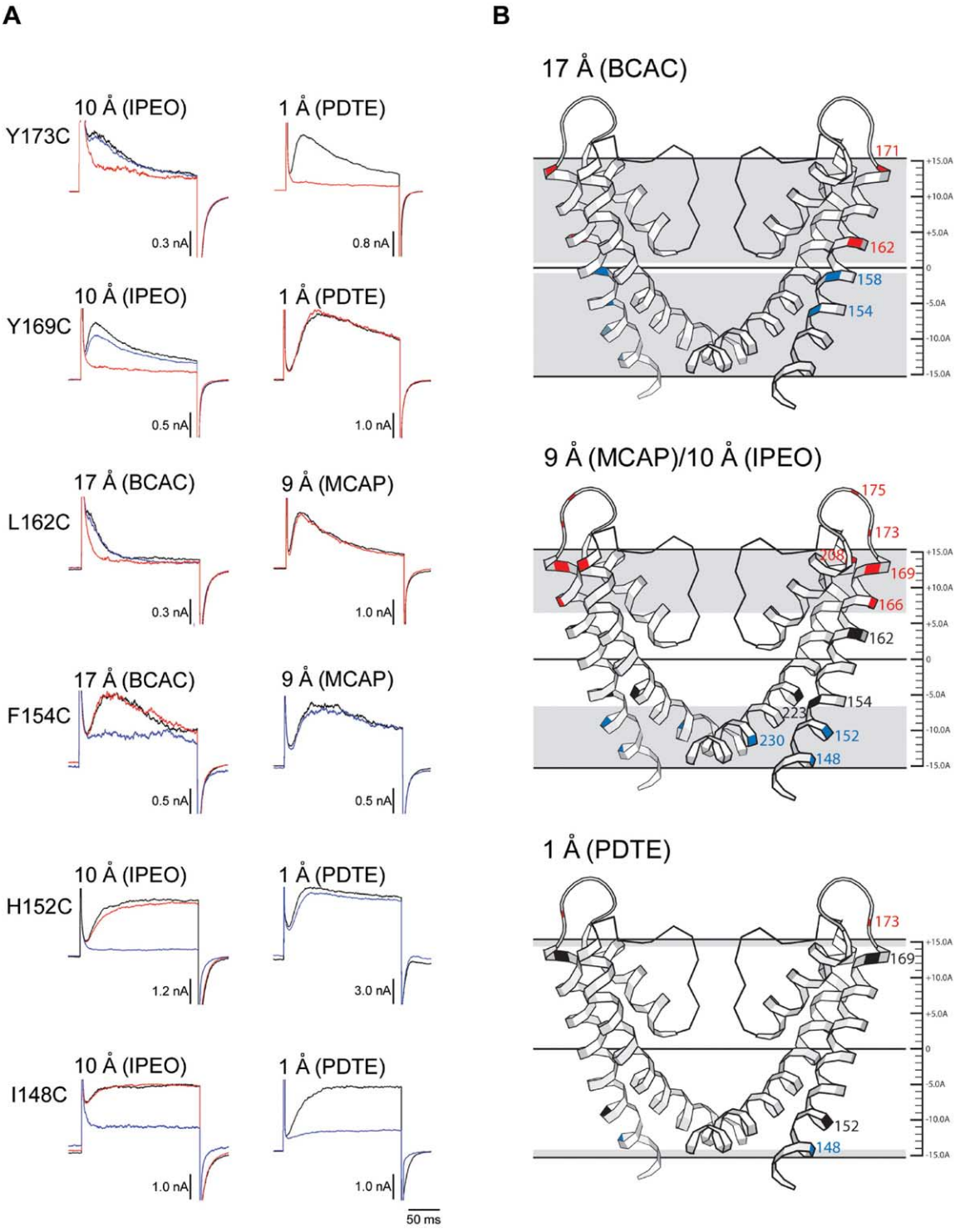

Figure 3. Calibration with the KvAP Pore

(A) Representative experiments showing the effects of avidin binding on S5 residues labeled with a longer (left) and shorter (right) biotin tether. Current traces were elicited with depolarizing steps in the absence (black traces) or presence of internal (blue traces) or external (red traces) avidin. Each current trace is the average of three to five measured traces.

(B) Accessibility of biotinylated residues mapped onto the pore structure. Red residues are accessible to only external avidin, blue residues are accessible to only internal avidin, and black residues are inaccessible to avidin. A 31 Å membrane is shown. Zones of accessibility for the different biotin reagents (17 Å deep, top panel; 9 Å deep, middle panel; 1 Å deep, bottom panel) are colored gray. Scale bar at right is in angstroms.

the Supplemental Data available with this article online). "Silent" binding of avidin without any consequence on channel function is unlikely in the context of the complete inhibition that occurs when avidin binds to H152C labeled with a longer biotin tether. We must conclude that the 1 Å (PDTE) tether attached to H152C is simply too short to allow biotin to reach its binding site in avidin in the intracellular solution.

F154C, lying even deeper beneath the surface of the membrane on the S5 helix, is able to bind intracellularly applied avidin but only when labeled with the 17 Å (BCAC) tether; the 9 Å (MCAP) biotin tether attached to F154C is too short to capture avidin in the internal solution. A similar pattern of differential accessibility to avidin is observed for residues near the C terminus of the S5 helix that are located at different distances from the external surface of the membrane (L162C, Y169C, and Y173C in Figure 3A.) The important point illustrated from this scan of residues within S5 is that avidin accessibility depends on the position of the residue within the helix and the length of the biotin tether (Figures 2A and 2B and 3A and 3B).

The accessibility data for the four biotin tethers is mapped onto the structure of the KvAP pore in Figure 3B. Data from channels labeled with the 9 Å (MCAP) and 10 Å (IPEO) biotin tethers have been grouped together due to the similar length of the tethers. Residues in Figure 3B are color coded according to their accessibility to avidin: red, external only; blue, internal only; and black, inaccessible. We observe an internally consistent pattern of accessible and inaccessible residues that is related to the membrane layer. How thick is the membrane as reported by these data? All S5 residues labeled with the 17 Å (BCAC) tether can bind avidin from one side of the membrane or the other but never from both sides. The minimum thickness of the membrane is defined by the accessibility of sites on the pore labeled with this longest biotin tether. M158C labeled with the 17 Å (BCAC) tether can only bind avidin in the internal solution and so must lie greater than 17 Å from the external surface of the membrane. Conversely, L162C labeled with the 17 Å (BCAC) tether can only bind avidin in the external solution and so must lie greater than 17 Å from the internal side of the membrane. M158 and L162 are separated by 5 Å. Therefore, the membrane as a barrier to avidin is minimally 29 Å thick (e.g., 2 × 17 Å − 5 Å). This conservative estimate assumes that residues L159–V161 would be accessible to avidin from both sides of the membrane when labeled with the 17 Å (BCAC) biotin tether.

The maximum thickness of the membrane is defined by the accessibility of Y173C labeled with the 1 Å (PDTE) tether to external avidin and the accessibility of I148C labeled with the 1 Å (PDTE) tether to internal avidin. These two residues are separated by 31 Å, and so the membrane as a barrier to avidin could be as thick as ~33 Å (e.g., 2 × 1 Å + 31 Å). Similar arguments can be worked through for different pairs of accessible and inaccessible residues on the KvAP pore labeled with the different tethers, but all arrive at the same essential conclusion: the boundaries of the lipid bilayer that exclude a large soluble protein like avidin are 29–33 Å apart. We cannot more fully constrain the membrane thickness only because we have not determined the accessibility of every site on the KvAP pore with every length of biotin tether.

How does this estimate of membrane thickness relate to known physical parameters of the lipid membrane? X-ray and neutron diffraction experiments show that the thickness of the hydrocarbon core of a fluid dioleoylphosphatidylcholine (DOPC) bilayer is ~29 Å (Wiener and White, 1992; Hristova and White, 1998), very close to our functional measurement for the fraction of the lipid bilayer that avidin cannot access. The correspondence of these two measurements makes physical sense: a soluble protein like avidin likely can penetrate much of the polar head-group layer of the lipid membrane but is excluded from its oily hydrocarbon core. Moreover, our estimate for the thickness of the membrane from the biotin-avidin accessibility data is in good agreement with the expected boundaries of the membrane's hydrophobic core suggested by the KvAP pore structure (Jiang et al., 2003a).

From these accessibility measurements of pore amino acids, this binary assay reports that the membrane is a barrier to avidin penetration and that the chemical distances of the different tethers in an extended conformation provide an accurate ruler to measure the thickness of the membrane's hydrocarbon core and the depth of amino acids within it. The use of different tether lengths has provided an internally consistent data set that tightly constrains the distance determination. These data provide a calibration with which we next investigate components of the voltage sensor.

The Voltage-Sensor Helices S1 and S2

We next determined the avidin accessibility of residues within the S1 and S2 helices of the voltage-sensor domain labeled with different-length biotin tethers (Figure S2). Several important aspects of the accessibility of residues in S1 and S2 are similar to what we observe in the pore. As in the pore, no residues in S1 or S2 are accessible to avidin from both sides of the membrane even when these residues are labeled with the longest biotin tether used. In fact, I67C lying in the middle of the S2 helix labeled with the 17 Å (BCAC) is inaccessible to avidin from either side of the membrane (Figure 2C). An explanation for this result is that the 17 Å (BCAC) tether is less than half the thickness of the membrane and that I67C labeled with this biotin tether lies squarely in a narrow region in the middle of the membrane that is unable to reach avidin in either the intracellular or extracellular solution. If this is true, the actual membrane thickness must be at least 34 Å, closer to the upper limit of our estimate based on the calibration with the KvAP pore.

However, more significant than the accessibility of any single site is the overall coherent pattern of avidin accessibility that emerges from studying multiple sites along the length of the S1-S2 helices labeled with the different biotin tethers. In Figure 4, amino acids on the S1 and S2 helices of the voltage sensor are labeled according to the color scheme used for accessibility of pore amino acids. The basic correspondence of the pattern of avidin accessibility for residues in the S1 and S2 helices with residues in the pore allows for two im-

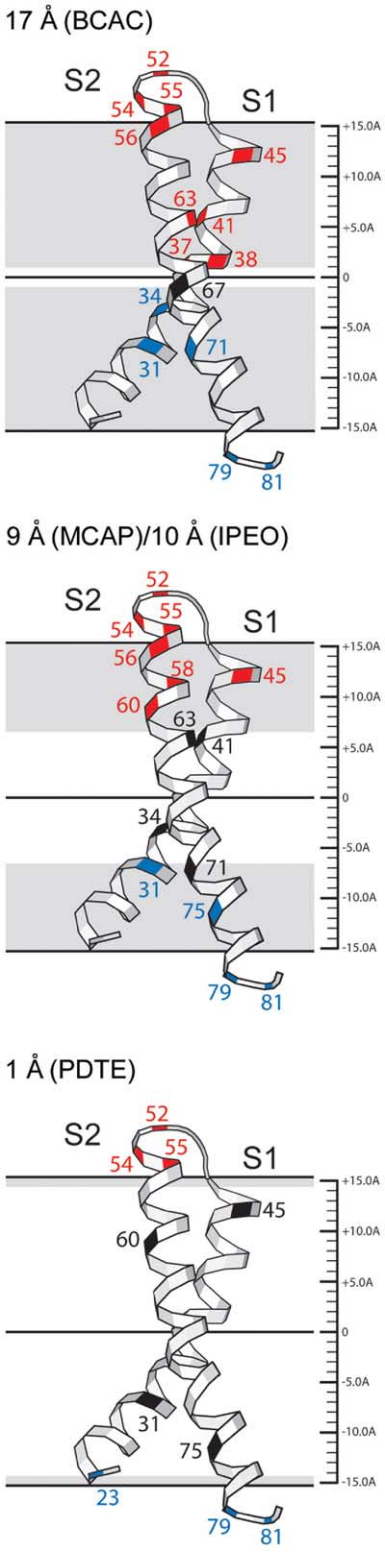

Figure 4. Accessibility of Amino Acids on the S1 and S2 Helices of the Voltage Sensor

S1 and S2 helical segments from the crystal structure of the KvAP isolated voltage-sensor domain are positioned within the membrane boundaries and zones of accessibility (gray regions) derived from the calibration with the pore. Red residues are accessible to only external avidin, blue residues are accessible to only internal avidin, and black residues are inaccessible to avidin. Scale bar at right is in angstroms.

portant conclusions. First, the membrane thickness as a barrier to avidin defined by the accessibility of residues within the S1 and S2 helices is consistent with our estimate derived from the KvAP pore. Second, the S1 and S2 helices, like the helices of the pore, apparently do not undergo large displacements perpendicular to the membrane plane (see below).

The Voltage-Sensor Paddle

If the large translational motion of the voltage-sensor paddle is true, we should find a very different pattern of avidin accessibility for residues in the paddle (the helical hairpin formed by S3b and S4) in comparison with stationary regions of the channel (Figure S3). Figure 5 summarizes the avidin accessibility of residues within the voltage-sensor paddle from G101C on the S3b segment to I127C on the S4 segment and maps the data onto the helical hairpin structure. Positions assayed for avidin accessibility are color coded in Figure 5B as in previous figures. However, now a new color must be introduced specifically for residues on the voltage-sensor paddle. Yellow residues on the paddle represent a class of accessible sites not seen anywhere else on the channel, residues that can bind avidin from both sides of the membrane. The accessibility of biotinylated residues on the voltage-sensor paddle is unique and unlike what is observed for residues in the pore or the S1 and S2 helices of the voltage sensor in several respects, which we consider below.

From the calibration with the pore, S1, and S2, we know that residues labeled with the 1 Å (PDTE) biotin tether must lie very close to the membrane surface in order to be accessible to avidin. Avidin in the extracellular solution can capture biotinylated residues on the tip of the paddle and on the first helical turn of S4 including L118C (Figure 5A). Just two helical turns away on S4, L125C labeled with the 1 Å (PDTE) tether binds avidin from the internal side of the membrane (Figure 5A). Remarkably, L118 and L125 are separated by just 10 Å on the S4 helix. Recall that the closest residues labeled with the 1 Å (PDTE) tether on the KvAP pore that bind avidin from opposite sides of the membrane are 31 Å apart. Because avidin cannot penetrate the membrane, the only explanation for the accessibility of these two nearby residues on S4 is to invoke that the voltage-sensor paddles move through the membrane to bring L125C within ~1 Å of the internal membrane boundary and L118C within ~1 Å of the external membrane boundary in different gating states of the channel (Figure 5B, bottom panel). To account for the accessibility of biotinylated sites on S4 labeled with the 1 Å (PDTE) tether, this region of the paddle must move a minimum of 17 Å perpendicular to the plane of the membrane, assuming the minimum membrane thickness of 29 Å. If the membrane is actually 34 Å thick, the displacement of this portion of the S4 segment will be 22 Å.

The large displacement of the S4 segment suggested by the accessibility data using the 1 Å (PDTE) biotin tether predicts that there should be multiple residues on S4 that are accessible to avidin from both sides of the membrane when labeled with the longer biotin tethers. In a previous study, we found that two residues

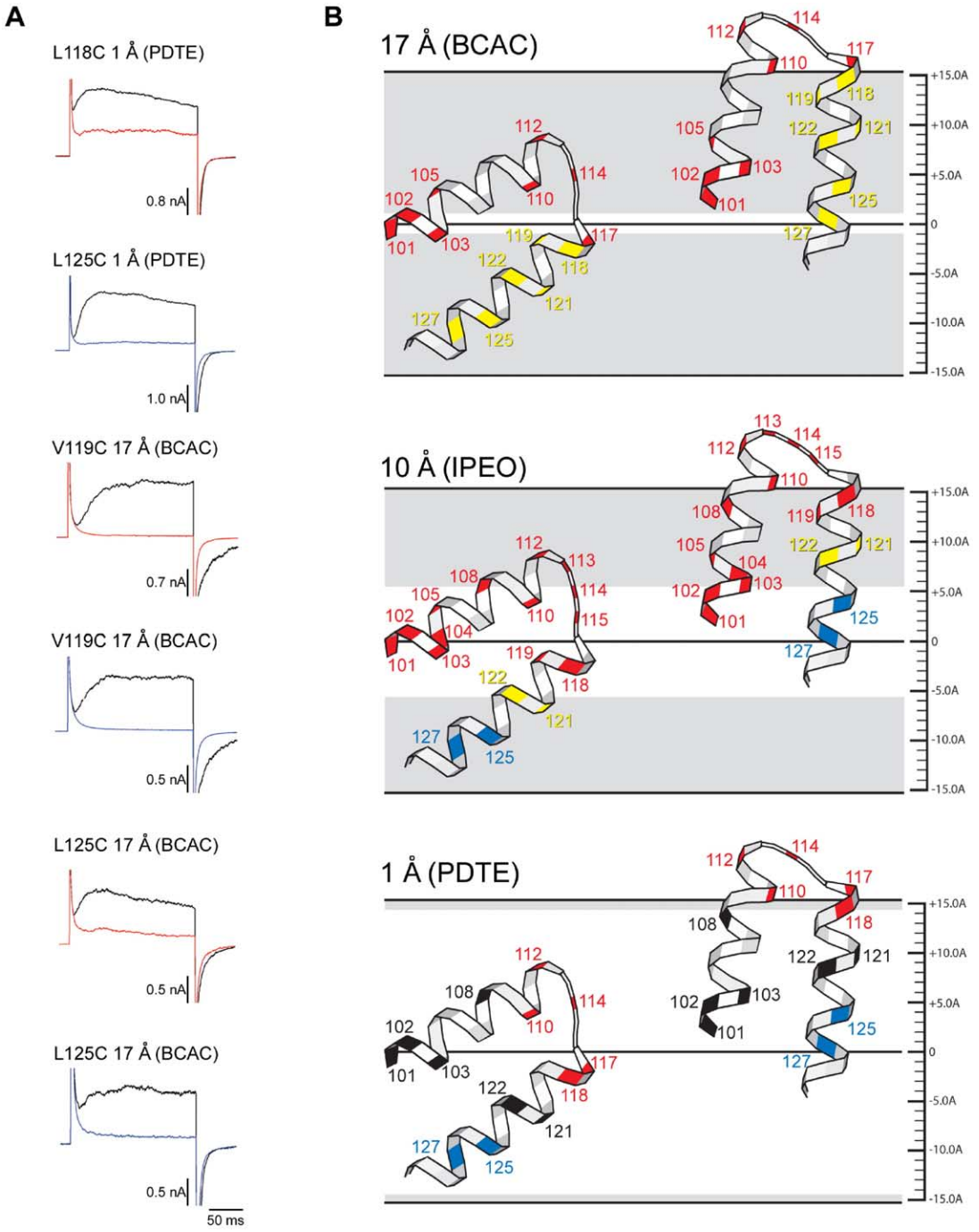

Figure 5. Accessibility of Voltage-Sensor-Paddle Residues Invokes Motion

(A) Representative experiments showing the effects of avidin on paddle residues labeled with the indicated biotin tether. Traces show averaged currents in response to depolarizing steps prior to (black) and after addition of external (red) or internal (blue) avidin.

(B) Depth of the voltage-sensor paddle within the membrane in the closed (left) and opened (right) conformation of the channel, positioned according to the constraints of the biotin-avidin accessibility data. The membrane boundaries are derived from the calibration with the pore. Zones of accessibility for the different biotin reagents derived from the pore, S1, and S2 are colored gray and extrapolated to the 10 Å biotin tether (middle panel) since the 9 Å tether was not used to label paddle residues. Red residues are accessible to only external avidin, blue residues are accessible to only internal avidin, black residues are inaccessible, and yellow residues are accessible to avidin from both sides of the membrane. Scale bar at right is in angstroms.

within the S4 segment (L121C and L122C), when labeled with the 10 Å (IPEO) biotin tether, are in fact able to grab avidin in the solution on both sides of the membrane (Jiang et al., 2003b) (Figure 5B, middle panel). We can now understand the dual accessibility of these two residues on S4 in the context of the accessibility of resi-

dues elsewhere on the channel. In the KvAP pore and the S1-S2 helices of the voltage sensor, we find that no sites are accessible to avidin from both sides of the membrane even when labeled with the longer 17 Å (BCAC) biotin tether. The dual accessibility of residues labeled with a 10 Å biotin tether exclusively in S4 substantiates our previous conclusion that movement of the S4 segment is large and can actually drag the bulky 10 Å (IPEO) biotin tether fully through the lipid membrane as the channel gates. The accessibility data using the 10 Å (IPEO) tether indicate that the S4 segment translates between 11–21 Å as the channel moves from a closed to an opened conformation. This estimate for the paddle displacement has a broader range due to the granularity of the measurement—the accessibility of every residue on S4 labeled with the 10 Å (IPEO) biotin tether was not determined.

The pattern of accessibility for residues on the voltage-sensor paddle labeled with the 10 Å (IPEO) tether is unique in another respect. All residues on S3b and S4 are accessible to avidin from one side of the membrane or the other when labeled with the 10 Å (IPEO) biotin tether. In comparison, on the pore, S1, and S2, we find multiple residues that are inaccessible to avidin on either side of the membrane when labeled with this biotin tether or the similar-length 9 Å (MCAP) biotin tether. Again, this suggests that the voltage-sensor paddle must undergo a sizable motion in order to bring the α-carbon of all residues within 10 Å of either the internal or external membrane boundary.

Consistent with the large displacement of the S4 segment, we find a region of S4 spanning at least 10 residues that can bind avidin from both sides of the membrane when labeled with the 17 Å (BCAC) tether (L118–I127, Figure 5B, top panel). For these residues, avidin addition to either side of the membrane resulted in complete inhibition (Figure 5A). In contrast to the dual accessibility of residues in the voltage-sensor paddle, no sites on the pore, S1, or S2 were found to be accessible to both external and internal avidin when labeled with the 17 Å (BCAC) biotin tether. In fact, a residue in the middle of S2 biotinylated with the 17 Å tether is unable to reach avidin from either side of the membrane. This result indicates that much of the S4 helix must move fully between the lower and upper membrane leaflet during channel gating.

The large motion of the voltage-sensor paddle has been derived in this study independently of any considerations of the gating state of the channel that we are measuring. We have used the robust binary measure of accessibility or inaccessibility to avidin alone to deduce the motion of the voltage-sensor paddles relative to the surface of the membrane. However, the motion of the paddle depicted in Figure 5B implies that most sites labeled with the shorter biotin tethers will be able to reach avidin only in some gating states of the channel and not in others and, therefore, avidin binding will depend on membrane voltage. Consistent with this idea, all externally accessible residues labeled with the 10 Å (IPEO) biotin tether were shown to require membrane depolarization to allow avidin binding to occur and could be protected from binding by holding the channel closed with negative membrane voltages (Jiang et al., 2003b). As expected, externally accessible residues labeled with the shorter 1 Å (PDTE) biotin tether similarly show state-dependent accessibility to extracellular avidin (Figure 2E). This state dependence is due to the length of the biotin tether because when the same paddle residues are labeled with the longer 17 Å tether, avidin can bind prior to membrane depolarization (Figure 2E).

Discussion

The accessibility data using avidin capture of biotinylated channels indicate that the voltage-sensor paddle is uniquely mobile compared to other regions of the ion channel and that the conserved S4 arginine residues move 15–20 Å through the thickness of the membrane. Even if local crevices or deformations of the lipid membrane near the transmembrane helices exist, because avidin is so large, it would be unable to penetrate into such regions (Figure 1B). Therefore, there is no escaping the basic conclusion that the mobile regions of the voltage sensor are moving 15 to 20 Å in the biotin-avidin accessibility assay.

However, one caveat that we must consider is the following: could it be that such large motions result in this assay because extreme conformations of the sensor are captured due to the nearly irreversible binding of biotin to avidin? Several aspects of the data suggest that it is unlikely that avidin is capturing rare conformations or fluctuations of the channel in the membrane. If it were, first of all, it would be very difficult to explain the observed pattern of accessibilities for the pore, S1, and S2, which are quantitatively consistent with the extended linker lengths and the known membrane bilayer thickness (Wiener and White, 1992; Hristova and White, 1998) (Figures 1, 3, and 4). Of course, one could still argue that the pore, S1, and S2 are static components of the channel and that capture of rare conformations will only involve intrinsically mobile components of the channel, that is, that the voltage-sensor paddle is mobile and has the capacity to undergo large movements but does not normally do so. The data point against this interpretation: there are sharp transitions between accessible and inaccessible positions on the voltage-sensor paddle and elsewhere (Figures 2C and 2D). Capture of rare conformations due to thermal fluctuations of the protein would be expected to follow some reasonably continuous distribution along a helix (i.e., if a given position is captured readily by avidin, nearby sites should also exhibit some measurable capture), but what we observe instead are positions separated by a single amino acid on S4 going from full reactivity by the first depolarization to no reactivity over 30 min (Figure 2D). Such sharp transitions are completely inconsistent with the idea that avidin is capturing rare conformations. Finally, and perhaps most importantly, the state-dependent accessibility of paddle residues labeled with the shorter biotin tethers indicates that avidin binding is coupled to channel opening (Figure 2E) (Jiang et al., 2003b). Based on these aspects of the data, it is likely that the data presented here reflect the true depth of amino acid positions within the membrane and the changes in depth that occur in association with gating of the Kv channel.

How do the large voltage-sensor movements deduced in this study of KvAP compare with movements deduced using other techniques applied to other Kv channels? In addition to the biotin-avidin method used here, three predominant approaches have been used to estimate the sensor motion in Kv channels: accessibility of site-directed cysteine residues to small thiol-reactive compounds (Mannuzzu et al., 1996; Larsson et al., 1996; Yusaf et al., 1996; Baker et al., 1998), accessibility of inhibitory spider toxins to the voltage sensor (Phillips et al., 2005), and fluorescence or luminescence resonance energy transfer (FRET or LRET) changes associated with gating (Glauner et al., 1999; Cha et al., 1999; Posson et al., 2005). As discussed earlier, the pervasive state-dependent accessibility of cysteine residues on S4 to thiol-reactive compounds is subject to two possible interpretations, one of which is in good quantitative agreement with the large conformational changes deduced from the biotin-avidin accessibility measurements. The ability of spider toxins to bind to both the closed and open conformation of the voltage sensor has been argued by Swartz and colleagues to be evidence that the voltage sensor does not undergo very large movements (Phillips et al., 2005), but their argument is not supported by the data. The voltage-sensor toxins insert into the outer leaflet of the lipid membrane (Lee and MacKinnon, 2004; Suchyna et al., 2004), and they interact with residues on S3 (Swartz and MacKinnon, 1997), which remains in the membrane's outer leaflet (Figure 5B). Furthermore, S3 in Kv2.1—the channel in which most of the toxin studies have been carried out—most likely extends for nearly two additional helical turns toward the extracellular surface compared to S3 in KvAP (based on the crystal structure of Kv1.2; Long et al., 2005a). The spider-toxin data are indeed completely compatible with the kind of voltage-sensor-paddle depth changes shown in Figure 5B.

We can not reconcile the accessibility data presented here with the LRET data, which have led Bezanilla, Selvin, and colleagues to conclude that the voltage sensor undergoes transverse movements no greater than 2.0 Å (Cha et al., 1999; Posson et al., 2005). However, several aspects of the LRET data lead us to wonder exactly what distances are being measured in those studies, especially since we now have determined a crystal structure of a Shaker family channel, Kv1.2, with which to evaluate their method (Long et al., 2005a). First, the absolute distance measured between equivalent S4 positions on adjacent subunits using LRET does not agree with the crystal structure (e.g., Shaker V363 by LRET was reported to be 32 Å; the equivalent residue on Kv1.2, V295, by crystallography is 48 Å) (Cha et al., 1999; Long et al., 2005b). Second, when the caged Tb^{3+} in the LRET studies is moved to different positions on the voltage sensor—which, according to the Kv1.2 crystal structure, should be at very different distances relative to the pore—little variation in distance (to a reference toxin) by LRET is observed (Posson et al., 2005), suggesting a lack of sensitivity in the LRET assay especially as the distances become longer. In the biotin-avidin accessibility studies presented here, we have distributed "probes" over the entire channel protein in order to use regions of known structure to calibrate our method. We suggest that similarly rigorous controls be carried out to determine the true range of accurate distance measurement allowed by the LRET method in a membrane bound Kv channel.

How do the physical distances of movement deduced in the present study correlate with electrical measurements in Kv channels? In the Shaker Kv channel, the first four arginines distributed along the S4 segment account for most of the channel's measured gating charge (Aggarwal and MacKinnon, 1996; Seoh et al., 1996). Displacement of the KvAP paddle as shown (Figure 5B) would enable 3 of the 4 conserved arginine guanidinium groups (R120, R123, and R126) to approach the intracellular phospholipid head-group layer in the closed ("down") position and 3 out of 4 (R117, R120, and R123) to approach the extracellular phospholipid head-group layer in the opened ("up") position if one takes into account the length of the arginine side chain. These large motions are nicely consistent with experiments in the Shaker channel showing that each of the first 4 S4 arginine residues contributes approximately 1 elementary charge unit to the gating charge (Schoppa et al., 1992; Aggarwal and MacKinnon, 1996; Seoh et al., 1996).

In contrast to the large displacement of the S4 segment, S3b never descends beneath the midpoint of the membrane. Even in the closed conformation, S3b remains in the membrane's outer leaflet, closer to the extracellular solution, and we imagine that, when it is down (closed), it causes the membrane to dimple, or distort locally, so that lipid-head groups and water molecules remain "above" it (and the disordered loop between S3 and S4 in some Kv channels would remain in the extracellular solution; Long et al., 2005a). This would account for the accessibility of small thiol reagents to cysteine residues on S3b even in the closed conformation (Gandhi et al., 2003; Gonzalez et al., 2005). Could S3b and S4 open to some extent during gating? The biotin-avidin data do not preclude this possibility, but they are reasonably consistent with the rigid-body motion presented in Figure 5B. On this point, we note that the region of accessibility with the 10 Å (IPEO) linker covers 3.5 helical turns on S3b versus up to only 2 helical turns everywhere else (intracellular and extracellular sides of S1, S2, and S5) (Figure 5). This observation, together with the state dependence of many sites on S3b with the shorter linkers (Figure 2E) (Jiang et al., 2003b), leads us to conclude that S3b changes its depth substantially in the membrane. Furthermore, we have not observed a deviation from the helical hairpin conformation in numerous crystal structures (Jiang et al., 2003a; Lee et al., 2005). Therefore, until we obtain data that indicate otherwise, we propose that S4 moves as part of a voltage-sensor paddle (an antiparallel helix with S3).

X-ray crystallographic studies of a mammalian member of the Shaker Kv channel family (Kv1.2) have recently revealed a native structure of the voltage sensors in an open conformation (Long et al., 2005a). New crystal structures of the KvAP channel, combined with biochemical studies, suggest that KvAP is very similar to Kv1.2 in its native three-dimensional structure (Lee et al., 2005). Figure 6 shows a model of one subunit of KvAP based on these new data. A key feature of this

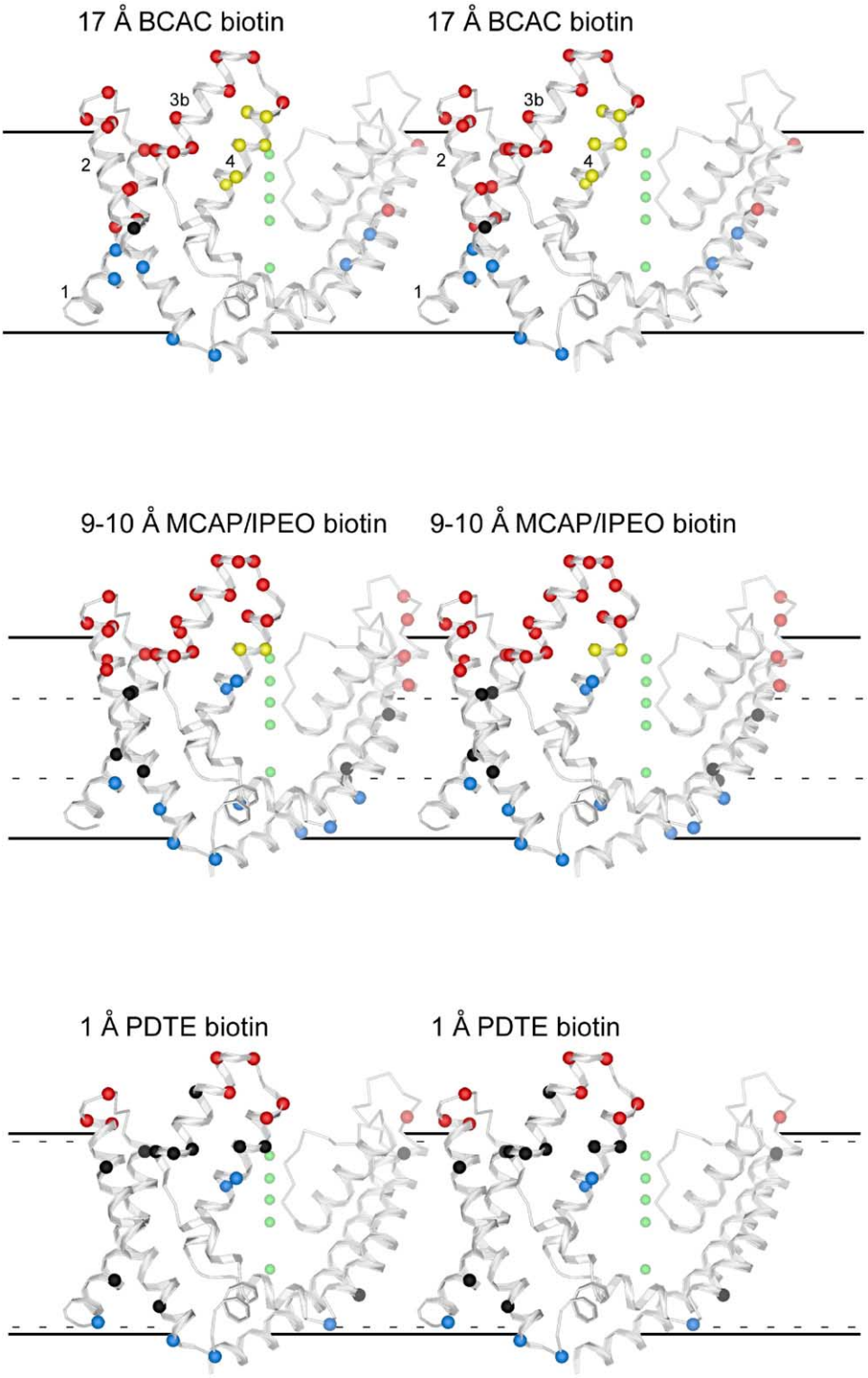

Figure 6. Summary of the Biotin-Avidin Accessibility Data

Stereo view of a single subunit of KvAP with accessibility data mapped onto the model (Lee et al., 2005). Membrane boundaries (solid lines) and zones of accessibility (hatched lines) are derived from calibration with the KvAP pore and S1 and S2 segments of the voltage sensor. Numbers in the upper panel mark the helical segments S1, S2, S3b, and S4. Each amino acid evaluated is represented as a colored sphere. Red residues are accessible to only external avidin, blue residues are accessible to only internal avidin, black residues are inaccessible, and yellow residues are accessible to avidin from both sides of the membrane.

model is that the voltage sensors are mechanically coupled to the pore through a single helix, the S4-S5 linker helix, but otherwise the sensors make very little contact with the pore. Consequently, the voltage sensors are suspended in the membrane as essentially independent domains. This fascinating feature of the structure probably explains why it has been possible to attach with impunity bulky biotin tethers throughout the voltage sensor (S1–S4) and S5: a channel with separate voltage-sensor domains surrounding the pore creates a large protein surface area exposed to the lipid membrane into which the biotin tethers can project.

The biotin-avidin accessibility data mapped onto the KvAP model in Figure 6 convey the following important information. The pattern of accessibility for the different biotin reagents on S1, S2, and S5 emphasizes that this assay accurately measures the depth of an amino acid inside the hydrophobic core of the membrane. The only rational interpretation of these data is that S1, S2, and S5 are static within the membrane with respect to transverse motion. In contrast, the charged region of S4 must move through a large fraction of the membrane's hydrophobic core. Its motion could be such that certain arginine residues on S4 could be stabilized in the open (Long et al., 2005b) and closed states by negative countercharges from the static S1 and S2 helices. It is easy to envision how a negative membrane voltage (negative inside), by exerting a force on the positive gating-charge arginines, would draw the mobile paddle inward to position the blue and yellow residues on S4 close to the same membrane depth as blue residues on S1, S2, and the pore, a translation of 15–20 Å. Depolarization of the membrane (positive inside) would exert an outward force on the arginines, causing the mobile paddle to adopt a position something like that shown in Figure 6, with the red and yellow residues on the paddle aligned with the red residues on S1, S2, and the pore. These motions would directly influence the position of the S4-S5 linker and hence the S6 inner helix of the pore (Long et al., 2005b).

The most important conclusion from the biotin-avidin accessibility experiments presented here is that the voltage-sensor paddle is distinctively mobile. The accessibility of biotinylated residues on the KvAP S4 segment is fully compatible with previous accessibility studies of eukaryotic Kv channels using small thiol-reactive compounds but allows for only one interpretation. In response to membrane depolarization, the movement of the voltage-sensor paddle translates the S4 segment and its gating-charge residues 15 to 20 Å across the membrane to bring about pore opening.

Experimental Procedures

Preparation of Reconstituted Biotinylated Channels

All accessibility studies were carried out using a KvAP channel in which the single endogenous cysteine was mutated to serine (C247S). Single cysteine mutations were introduced onto the KvAP C247S background channel using the QuikChange method (Stratagene) and confirmed by sequencing the entire gene. Mutant channels were expressed and purified as described (Ruta et al., 2003) except that, prior to gel filtration, mutant KvAP channels were incubated with 1 mM Tri(2-carboxyethyl)phosphine hydrochloride (TCEP) for 1 hr. Immediately after gel filtration, mutant channels (at 0.5–1.0 mg/ml) were incubated with either 4 mM PDTE biotin (biotin-[2-(2-pyridyldithio)ethylamide], Toronto Research Chemicals, Inc.), 4 mM MCAP biotin (N-biotinylcaproylaminoethyl methanethiosulfonate, Toronto Research Chemicals, Inc.), 4 mM IPEO biotin ((+)-biotinyl-iodoacetamidyl-3, 6-dioxaoctanediamine, Pierce), or 2 mM BCAC biotin (biotinylcaproylaminocaproylaminoethyl methanethiosulfonate, Toronto Research Chemicals, Inc.) at room temperature for 4–5 hr. Biotinylated channels were reconstituted into lipid vesicles as described (Heginbotham et al., 1999) to give a final protein concentration of between 0.8 and 1.2 mg ml^{-1}.

Gel shift assays were performed by adding either avidin (~5- to 10-fold molar excess) or an equal volume of buffer to aliquots of reconstituted biotinylated channels. SDS-containing sample buffer was then added to lyse vesicles and prevent underestimation of biotinylation due to the sidedness of channel orientation within vesicles. The extent of avidin-channel-complex formation was then analyzed by SDS-PAGE.

Electrophysiology

Electrophysiology of biotinylated KvAP channels was performed as described (Ruta et al., 2003). Biotinylated channels were incorporated into planar membranes and studied using various voltage protocols prior to and after addition of 40–100 μg/ml avidin (Pierce) to the solution on one side of the membrane. For most biotinylated channels, the effects of avidin binding on channel function were evaluated with 200 ms depolarizing pulses to +100 mV from a holding voltage of –100 mV repeated every 120 s. Some biotinylated channels exhibited shifted voltage-dependent activation and required more strongly negative holding voltages (up to –150 mV) or more strongly positive depolarizing voltages (up to +200 mV). Also, some biotinylated channels showed more rapid recovery from inactivation and could be tested with depolarizing pulses as frequently as every 30 s.

Supplemental Data

Supplemental Data include three figures and can be found with this article online at http://www.cell.com/cgi/content/full/123/2/463/DC1/.

Acknowledgments

We thank Francis Valiyaveetil for helpful discussion. This work was supported in part by a National Institutes of Health (NIH) grant to R.M. R.M. is an Investigator in the Howard Hughes Medical Institute.

Received: July 18, 2005
Revised: August 24, 2005
Accepted: August 31, 2005
Published: November 3, 2005

References

Aggarwal, S.K., and MacKinnon, R. (1996). Contribution of the S4 segment to gating charge in the Shaker K^+ channel. Neuron *16*, 1169–1177.

Baker, O.S., Larsson, H.P., Mannuzzu, L.M., and Isacoff, E.Y. (1998). Three transmembrane conformations and sequence-dependent displacement of the S4 domain in Shaker K^+ channel gating. Neuron *20*, 1283–1294.

Bezanilla, F. (2000). The voltage sensor in voltage-dependent ion channels. Physiol. Rev. *80*, 555–592.

Cha, A., Snyder, G.E., Selvin, P.R., and Bezanilla, F. (1999). Atomic scale movement of the voltage-sensing region in a potassium channel measured via spectroscopy. Nature *402*, 809–813.

Gandhi, C.S., and Isacoff, E.Y. (2002). Molecular models of voltage sensing. J. Gen. Physiol. *120*, 455–463.

Gandhi, C.S., Clark, E., Loots, E., Pralle, A., and Isacoff, E.Y. (2003). The orientation and molecular movement of a K^+ channel voltage-sensing domain. Neuron *40*, 515–525.

Glauner, K.S., Mannuzzu, L.M., Gandhi, C.S., and Isacoff, E.Y. (1999). Spectroscopic mapping of voltage sensor movement in the Shaker potassium channel. Nature *402*, 813–817.

Gonzalez, C., Morera, F.J., Rosenmann, E., Alvarez, O., and Latorre, R. (2005). S3b amino acid residues do not shuttle across the bilayer in voltage-dependent Shaker K^+ channels. Proc. Natl. Acad. Sci. USA *102*, 5020–5025.

Heginbotham, L., LeMasurier, M., Kolmakova-Partensky, L., and Miller, C. (1999). Single *Streptomyces lividans* K^+ channels. Functional asymmetries and sidedness of proton activation. J. Gen. Physiol. *114*, 551–560.

Hille, B. (2001). Ion Channels of Excitable Membranes (Sunderland, MA: Sinauer Associates, Inc.).

Hristova, K., and White, S.H. (1998). Determination of the hydrocarbon core structure of fluid dioleoylphosphocholine (DOPC) bilayers by x-ray diffraction using specific bromination of the double-bonds: effect of hydration. Biophys. J. *74*, 2419–2433.

Jiang, Y., Lee, A., Chen, J., Ruta, V., Cadene, M., Chait, B., and MacKinnon, R. (2003a). X-ray structure of a voltage-dependent K^+ channel. Nature *423*, 33–41.

Jiang, Y., Ruta, V., Chen, J., Lee, A., and MacKinnon, R. (2003b). The principle of gating charge movement in a voltage-dependent K^+ channel. Nature *423*, 42–48.

Larsson, H.P., Baker, O.S., Dhillon, D.S., and Isacoff, E.Y. (1996). Transmembrane movement of the Shaker K^+ channel S4. Neuron *16*, 387–397.

Lee, S.Y., and MacKinnon, R. (2004). A membrane-access mechanism of ion channel inhibition by voltage sensor toxins from spider venom. Nature *430*, 232–235.

Lee, S.Y., Lee, A., Chen, J., and MacKinnon, R. (2005). Structure of the KvAP voltage-dependent K+ channel and its dependence on the lipid membrane. Proc. Natl. Acad. Sci. USA *102*, 15441–15446.

Long, S.B., Campbell, E.B., and MacKinnon, R. (2005a). Crystal structure of a mammalian voltage-dependent Shaker family K^+ channel. Science *309*, 897–903. Published online July 7, 2005. 10.1126/science.1116269

Long, S.B., Campbell, E.B., and MacKinnon, R. (2005b). Voltage sensor of Kv1.2: structural basis of electromechanical coupling. Science *309*, 903–908. Published online July 7, 2005. 10.1126/science.1116270

Mannuzzu, L.M., Moronne, M.M., and Isacoff, E.Y. (1996). Direct physical measure of conformational rearrangement underlying potassium channel gating. Science *271*, 213–216.

Phillips, L.R., Milescu, M., Li-Smerin, Y., Mindell, J.A., Kim, J.I., and Swartz, K.J. (2005). Voltage-sensor activation with a tarantula toxin as cargo. Nature *436*, 857–860.

Posson, D.J., Ge, P., Miller, C., Bezanilla, F., and Selvin, P.R. (2005). Small vertical movement of a K^+ channel voltage sensor measured with luminescence energy transfer. Nature *436*, 848–851.

Pugliese, L., Coda, A., Malcovati, M., and Bolognesi, M. (1993). Three-dimensional structure of the tetragonal crystal form of egg-white avidin in its functional complex with biotin at 2.7 Å resolution. J. Mol. Biol. *231*, 698–710.

Qiu, X.Q., Jakes, K.S., Kienker, P.K., Finkelstein, A., and Slatin, S.L. (1996). Major transmembrane movement associated with colicin Ia channel gating. J. Gen. Physiol. *107*, 313–328.

Ruta, V., Jiang, Y., Lee, A., Chen, J., and MacKinnon, R. (2003). Functional analysis of an archaebacterial voltage-dependent K^+ channel. Nature *422*, 180–185.

Schoppa, N.E., McCormack, K., Tanouye, M.A., and Sigworth, F.J. (1992). The size of gating charge in wild-type and mutant Shaker potassium channels. Science *255*, 1712–1715.

Senzel, L., Huynh, P.D., Jakes, K.S., Collier, R.J., and Finkelstein, A. (1998). The diphtheria toxin channel-forming T domain translocates its own NH2-terminal region across planar bilayers. J. Gen. Physiol. *112*, 317–324.

Seoh, S.A., Sigg, D., Papazian, D.M., and Bezanilla, F. (1996). Voltage-sensing residues in the S2 and S4 segments of the Shaker K^+ channel. Neuron *16*, 1159–1167.

Sigworth, F.J. (1994). Voltage gating of ion channels. Q. Rev. Biophys. *27*, 1–40.

Slatin, S.L., Qiu, X.Q., Jakes, K.S., and Finkelstein, A. (1994). Identification of a translocated protein segment in a voltage-dependent channel. Nature *371*, 158–161.

Suchyna, T.M., Tape, S.E., Koeppe, R.E., Andersen, O.S., Sachs, F., and Gottlieb, P.A. (2004). Bilayer-dependent inhibition of mechanosensitive channels by neuroactive peptide enantiomers. Nature *430*, 235–240.

Swartz, K.J., and MacKinnon, R. (1997). Mapping the receptor site for hanatoxin, a gating modifier of voltage-dependent K^+ channels. Neuron *18*, 675–682.

Wiener, M.C., and White, S.H. (1992). Structure of a fluid dioleoylphosphatidylcholine bilayer determined by joint refinement of x-ray and neutron diffraction data. III. Complete structure. Biophys. J. *61*, 437–447.

Yang, N., and Horn, R. (1995). Evidence for voltage-dependent S4 movement in sodium channels. Neuron *15*, 213–218.

Yang, N., George, A.L., and Horn, R. (1996). Molecular basis of charge movement in voltage-gated sodium channels. Neuron *16*, 113–122.

Yusaf, S.P., Wray, D., and Sivaprasadarao, A. (1996). Measurement of the movement of the S4 segment during the activation of a voltage-gated potassium channel. Pflugers Arch. *433*, 91–97.